# Convection cells in thin electrolytic films

C. Anteneodo[a,*], E. Ramos de Souza[a,b], D. Gallez[c], P.M. Bisch[a]

[a]*Instituto de Biofísica, Universidade Federal do Rio de Janeiro, Rio de Janeiro, Brazil*
[b]*Centro Federal de Educação Tecnológica da Bahia, Salvador, Brazil*
[c]*Service de Chimie Physique and Centre for Nonlinear Phenomena and Complex Systems,
Université Libre de Bruxelles, Brussels, Belgium*

**Abstract**

The adhesion of biomembranes may display regular patterns even in the absence of specialized contact sites. In particular, recent experiments show that charged lipid vesicles adhere to an oppositely charged substrate forming blisters. Patterns in the thin aqueous electrolyte film confined between membranes can be appropriately described through an electro-hydrodynamics approach. By solving the corresponding equations numerically, we show that, when steady non-homogeneous patterns are established, the electrolyte flows in convective motion forming well structured cells. © 2000 Elsevier Science B.V. All rights reserved.

## 1. Introduction

The adhesion of lipid membranes has been the object of many recent studies [1–4]. Due to the interplay of repulsive and attractive nonspecific forces (electrostatic, van der Waals, hydration, macromolecular depletion or cross-bridge), adhesion structures characterized by spatially periodic contact points can arise. Patterning was detected in experiments with red blood cells [3]. Also, blistering on charged lipid giant vesicles, in the presence of a lipid substrate bearing opposite electric charge, was recently observed [4]. The common feature is the presence of a thin aqueous film delimited by membranes. These films are submitted to spatio-temporal instabilities that can lead to the formation of steady patterns [5,6].

---

* Corresponding author. Fax: 55-21-280-8193.
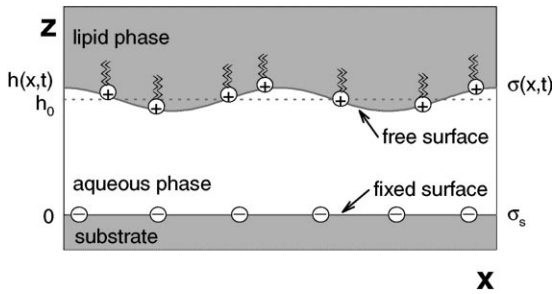*E-mail address:* celia@cbpf.br (C. Anteneodo)

Fig. 1. The system: a thin aqueous film bounded by a rigid substrate and by a free surface delimiting a lipid phase. The substrate and the free surface have electric charge densities of opposite sign ($\sigma_s$ and $\sigma$, respectively). The free surface is described by $z = h(x,t)$.

Having in mind these experiments, we used an electrohydrodynamics approach in order to model the thin aqueous film confined between a charged substrate and a fluid membrane with insoluble charged surfactants moving on the water–membrane interface. Evolution equations for the film thickness and for the concentration of the charged surfactant were derived from the Navier–Stokes and continuity equations [7]. The model satisfactorily describes the main experimentally observed features. Two qualitatively different steady state situations can arise: either a planar state with homogeneous charged surfactant concentration or a pattern with non uniform film thickness and inhomogeneous distribution of charged surfactant.

In the present work we focus on the motions of the aqueous fluid confined between the rigid substrate and the free water–membrane interface.

## 2. Electrohydrodynamics model

Let us consider a thin aqueous layer of mean thickness $h_0$, density $\rho$ and viscosity $\mu$, bounded by a fixed substrate and by a fluid membrane of density $\rho'$ and viscosity $\mu'$ (Fig. 1). The film thickness $h(x,t)$ is a function of the lateral coordinate $x$ and time $t$. Symmetry is assumed in the $y$ direction. The free surface is located at $z = h(x,t)$, $z$ being the normal coordinate. Charged surfactant molecules can move along the free interface with a lateral diffusion coefficient $D$. The substrate at $z = 0$ bears opposite electric charge $\sigma_s$. All quantities are appropriately dimensionless [7].

We consider that each fluid element is submitted to conservative body forces and that the interfaces are under electro-hydrodynamical normal and tangential stresses [8]. We assume that, at the free interface, the surface tension $\Sigma$ satisfies the linear equation of state $\Sigma = \Sigma_0 - \tilde{M}\sigma$, where $\sigma$ is the surface charge density, $\tilde{M} = -\partial\Sigma/\partial\sigma$ is the reduced Marangoni number, and $\Sigma_0$ is the surface tension in the absence of charged surfactant. The disjoining pressure $\phi$ takes into account the external electric force in

the aqueous phase as well as the normal electric stress [9]:

$$\phi(h,\sigma) = \left(\frac{8\pi}{\varepsilon}\right)\frac{\sigma^2 + \sigma\sigma_s(e^{\kappa h} + e^{-\kappa h}) + \sigma_s^2}{(e^{\kappa h} - e^{-\kappa h})^2},\tag{1}$$

where $\varepsilon$ is the aqueous phase dielectric constant and $\kappa$ is the inverse of the Debye length. The electric potential at the free surface, $\psi$, is given by [9]

$$\psi(h,\sigma) = \left(\frac{4\pi}{\varepsilon\kappa}\right)\frac{2\sigma_s + \sigma(e^{\kappa h} + e^{-\kappa h})}{e^{\kappa h} - e^{-\kappa h}}.\tag{2}$$

The two-dimensional motion inside the film is governed by Navier–Stokes equations for incompressible fluids. These equations as well as the corresponding boundary conditions can be considerably simplified since the wavelength of the film deformation $\lambda$ is far greater than the film thickness $h$. All quantities are first scaled on the small parameter $\eta = h/\lambda \ll 1$. After expanding the variables in perturbation series [8,10], the terms of lower order in $\eta$ are kept. The dimensionless expressions at zero order for the components of the velocity $\boldsymbol{v}$ inside the electrolyte film [7,11] result

$$u = \boldsymbol{v}\cdot\hat{x} = -M\sigma_x z + [\Sigma_0 h_{xx} + \phi]_x(-\tfrac{1}{2}z^2 + zh),\tag{3a}$$

$$v = \boldsymbol{v}\cdot\hat{y} = (M\sigma_x - [\Sigma_0 h_{xx} + \phi]_x h)_x z^2/2 + [\Sigma_0 h_{xx} + \phi]_{xx}z^3/6,\tag{3b}$$

where $M \equiv \tilde{M}/(1 - \mu'/\mu)$.

The evolution equation for the film thikness $h \equiv h(x,t)$ is obtained from the kinematic condition at the interface

$$v = h_t + uh_x.\tag{4}$$

Also, a conservation equation is adopted for $\sigma \equiv \sigma(x,t)$ which varies in time due to convective and diffusive effects [11]. The surface curvature is so large that changes of $\sigma(x,t)$ due to surface dilatation can be neglected. Then

$$\sigma_t = (D[\sigma_x + \sigma\psi_x] - \sigma u)_x.\tag{5}$$

## 3. Numerical results

A linear analysis was performed around the uniform steady state reference solution $(h,\sigma) = (h_0,\sigma_0)$. The resulting characteristic equation has two real roots. One of them is always negative, whereas the other one, $w^*$, does not have a definite sign. The system is asymptotically stable if $w^* < 0$ or unstable if $w^* > 0$, while marginal stability corresponds to $w^* = 0$. Then, the critical wavenumber $k_c$, for which $w^* = 0$, can be obtained [7]. The linear analysis puts into evidence that there are critical values of the parameters for the growth of instabilities, yielding two regimes: one where contact is homogeneous and another where blisters appear. Numerical integration of the evolution
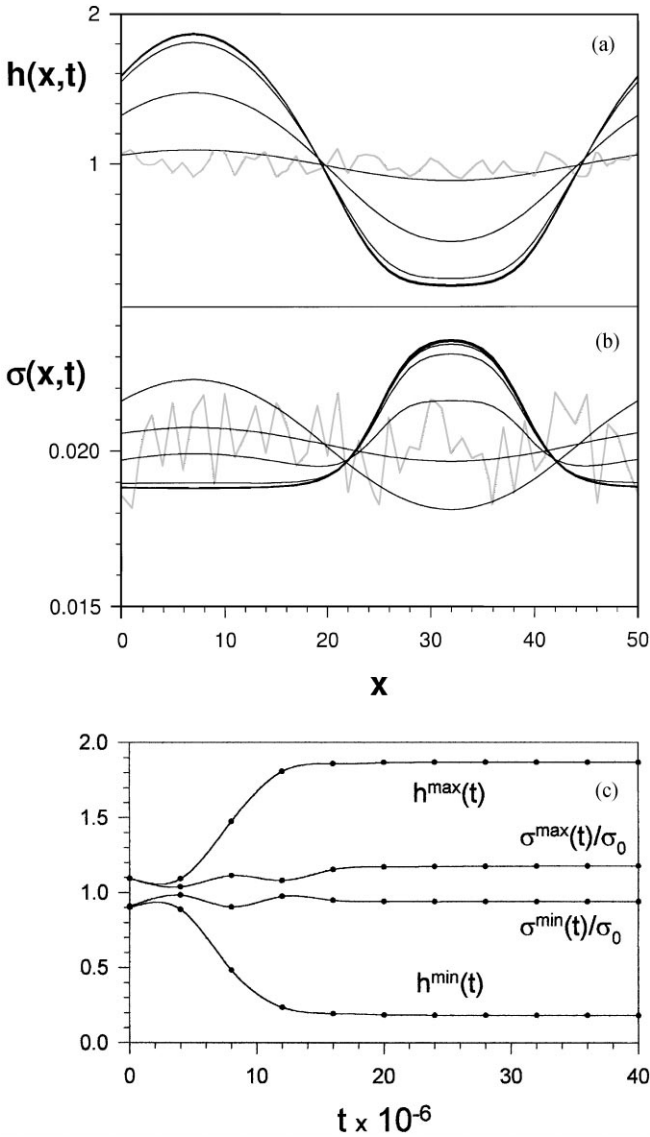
Fig. 2. Time evolution of the film surface $h(x,t)$ (a) and of the surface charge density $\sigma(x,t)$ (b), obtained from numerical integration of Eqs. (4) and (5), as a function of $x$ at various times $t$, starting from random initial conditions for $h(x,0)$ and $\sigma(x,0)$ (10% around the homogeneous state $h_0 = 1$, $\sigma_0 = 0.02$) at $t = 0$ (light gray), at intervals of $\Delta t = 4 \times 10^6$ up to $t = 4 \times 10^7$. The bounded domain with PBC is taken as $0 \leqslant x \leqslant L$, where $L = 50$. Integration was performed over a grid of 50 cells. (c) The temporal behavior of the minimal and maximal values of $h(x,t)$ and $\sigma(x,t)$ for stability control. Dimensionless parameters (chosen in the unstable domain) are $\sigma_s = -0.04$, $M = -10^{-4}$, $\Sigma_0 = 10^{-3}$, $D = 10^{-5}$ and $\kappa = \frac{10}{3}$.
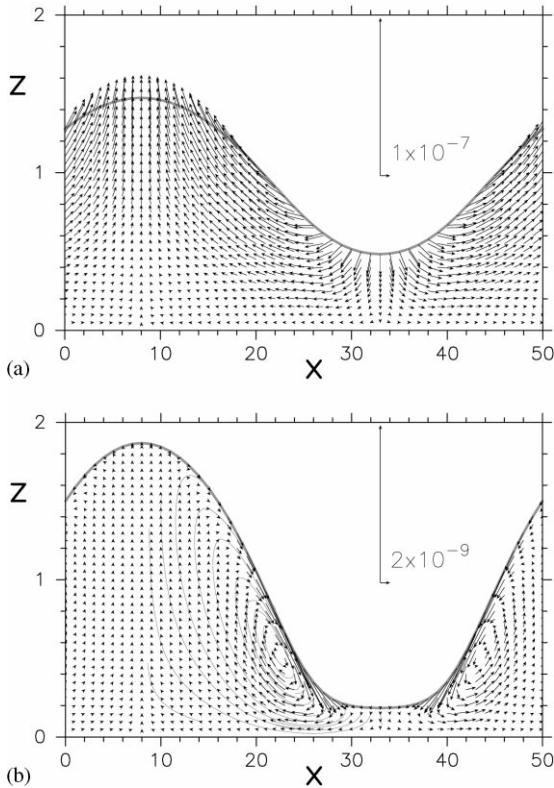
Fig. 3. Velocity field inside the aqueous film, from Eqs. (3), for the same parameter values as in Fig. 2, at times (a) $t = 1.2 \times 10^7$ and (b) $t = 2.4 \times 10^7$ (steady state attained). The magnitude and direction of the arrows indicate the values of the velocity field at the points from which the arrows are drawn. The scale for the intensity in each direction ($x$ and $z$) is shown in the figure. Some stream lines are represented in (b).

equations, performed for sets of parameters belonging to both domains, confirms the existence of those two regimes.

Eqs. (4) and (5) are solved as an initial value problem with spatially periodic bounded boundary conditions (PBC) by means of an FTCS finite difference scheme [12]. The bounded domain with PBC is taken as $0 \leqslant x \leqslant L$, where $L$ is chosen arbitrarily just requiring that $L > \lambda_c = 2\pi/k_c$. The shape of the film surface $h(x,t)$ as well as the profile of the vesicle charge density $\sigma(x,t)$, obtained from numerical integration, as a function of $x$ at various times $t$ are represented in Figs. 2a and b for parameters in the unstable domain. Fig. 2c shows the temporal behavior of the minimal and maximal values of $h(x,t)$ and $\sigma(x,t)$ followed for controlling the stability of the profiles.

In Fig. 3 we exhibit the velocity field for the same parameters in the unstable domain as in Fig. 2, at two different times: when patterns are being formed (a) and at the steady state (b).

## 4. Discussion

Since no-slip and no-penetration conditions are assumed, $v$ vanishes on the rigid interface, for all $t$. On the free interface, however, $v$ is not necessarily null. During the transient, water flows from the narrow regions of the film toward the broad regions (Fig. 3a), further enhancing the deformation. This picture stands qualitatively the same as far as the deformation keeps on growing. Once the steady state is attained, while the normal component vanishes on the interface (from the condition $h_t = 0$), the tangential one persists wherever the electrochemical gradient is not null, pointing toward the narrow regions. The tangential component only vanishes at the points where the width is an extreme since there the electrochemical gradient is null.

Fluxes surviving during the steady state are slow as compared to the velocity of deformation. Typical velocities during film evolution can be estimated from the time needed to reach the steady state ($\tau$) together with the mean thickness ($h_0$) and the mean size of the irregularities on the free interface ($\lambda$). Therefore, the $x$-component of the velocity, $u$, results between one and two orders larger than the $z$-component, $v$, since $u/v \simeq \lambda/h_0$. At the steady state, typical velocities are controlled by the diffusive effects which result in much smaller velocities than during the development of the perturbation.

Charged surface active molecules move along the interface due to diffusion following the electrochemical gradient and due to the action of forces originated from the adjacent fluid layers. In the steady state, both contributions balance and there is no net motion of surfactants. However, this balance does not occur for the interfacial fluid elements that keep on moving tangentially to the interface due to the action of the electrohydrodynamic forces. The change of orientation of the tangential velocity of fluid at the interface provokes the formation of structured cells (Fig. 3b). In other words, the competition between diffusion and migration of the charged surfactant along the free water–membrane interface induces a surface tension gradient that persists in the steady state and in turn originates convective patterns. From the biological point of view, these patterns could have interesting consequences on the interpretation of adhesion phenomena.

## References

[1] E. Sackmann, Science 271 (1996) 43.
[2] D.P. Pantazatos, R.C. MacDonald, Membrane Biol. 170 (1999) 27.
[3] D. Gallez, W.T. Coakley, Heterog. Chem. Rev. 3 (1996) 443.

[4] J. Nardi, T. Feder, T. Bruisma, E. Sackmann, Europhys. Lett. 37 (1997) 371.

[5] E. Ramos de Souza, D. Gallez, Phys. Fluids 10 (1998) 1804.

[6] T. Erneux, D. Gallez, Phys. Fluids 9 (1997) 1194.

[7] E. Ramos de Souza, C. Anteneodo, D. Gallez, P.M. Bisch, Long-scale evolution of thin liquid films bounded by a viscous layer with charged surfactants, preprint, 1999.

[8] A. Oron, S.H. Davis, S.G. Bankoff, Rev. Mod. Phys. 69 (1997) 931.

[9] V.A. Parsegian, D. Gingel, Biophys. J. 12 (1972) 1192.

[10] M.B. Williams, S.H. Davis, J. Coll. Int. Sci. 90 (1982) 220.

[11] A. De Wit, D. Gallez, I. Christov, Phys. Fluids 6 (1994) 3256.

[12] W.H. Press, S.A. Teukolsky, W.T. Vetterling, B.P. Flannery, Numerical Recipes in Fortran: The Art of Scientific Computing, Cambridge Universtiy Press, Cambridge, London, 1992.